International Journal of Pharmaceutics 655 (2024) 124034

Contents lists available at ScienceDirect

International Journal of Pharmaceutics

journal homepage: www.elsevier.com/locate/ijpharm

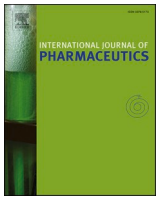

DIFUCOSIN: DIclofenac sodium salt loaded FUCOidan-SericIN nanoparticles for the management of chronic inflammatory diseases

Agnese Gagliardi [a], Emanuela Chiarella [b], Silvia Voci [a], Nicola Ambrosio [a], Marilena Celano [a], Maria Cristina Salvatici [c], Donato Cosco [a,*]

[a] Department of Health Sciences, University "Magna Græcia", 88100 Catanzaro, Italy
[b] Department of Experimental and Clinical Medicine, University "Magna Græcia", 88100 Catanzaro, Italy
[c] Institute of Chemistry of Organometallic Compounds (ICCOM)-Electron Microscopy Centre (Ce.M.E.), National Research Council (CNR), 50019, Sesto Fiorentino, Firenze, Italy

ARTICLE INFO

Keywords:
Diclofenac sodium
Fucoidan
Inflammatory diseases
Sericin
Nanoparticles

ABSTRACT

The current investigation emphasizes the use of fucoidan and sericin as dual-role biomaterials for obtaining novel nanohybrid systems for the delivery of diclofenac sodium (DS) and the potential treatment of chronic inflammatory diseases. The innovative formulations containing 4 mg/ml of fucoidan and 3 mg/ml of sericin showed an average diameter of about 200 nm, a low polydispersity index (0.17) and a negative surface charge. The hybrid nanosystems demonstrated high stability at various pHs and temperatures, as well as in both saline and glucose solutions. The Rose Bengal assay evidenced that fucoidan is the primary modulator of relative surface hydrophobicity with a two-fold increase of this parameter when compared to sericin nanoparticles. The interaction between the drug and the nanohybrids was confirmed through FT-IR analysis. Moreover, the release profile of DS from the colloidal systems showed a prolonged and constant drug leakage over time both at pH 5 and 7. The DS-loaded nanohybrids (DIFUCOSIN) induced a significant decrease of IL-6 and IL-1β with respect to the active compound in human chondrocytes evidencing a synergistic action of the individual components of nanosystems and the drug and demonstrating the potential application of the proposed nanomedicine for the treatment of inflammation.

1. Introduction

Inflammation can be defined as a double-edged sword. Indeed, it is a biological self-response designed to protect the body from injury or harmful endogenous and/or exogenous biophysico-chemical stimuli, characterized by orchestration of a wide range of molecular mediators and inflammatory cells (Liu et al., 2022a; Liu et al., 2022b). However, the failure of a pharmacological treatment may promote persistent tissue damage and a sustained inflammatory response lasting from months to years, a condition known as chronic inflammation (Dou et al., 2020). Among the chronic disorders, "inflammatory arthritis" is an umbrella term encompassing several conditions characterized by the inflammation of one or more articulations. It is a long-term disease that affects millions of people worldwide and causes pain, stiffness, and decreased mobility (Chapman et al., 2022).

Currently available first-line treatment options for this chronic disorder are non-steroidal anti-inflammatory drugs (NSAIDs) and glucocorticoids to control pain and inflammation and to prevent long-term joint erosion. However, the properties of these drugs have several drawbacks, the majority of which are related to reduced bioavailability and efficacy, poor water solubility, scarce cell uptake, unfavorable pharmacokinetics, random distribution *in vivo*, and degradation before reaching the target sites (Majumder and Minko, 2021; Zhang et al., 2022). Additionally, the new frontier in the treatment of these chronic pathologies is to combine biological agents with traditional disease-modifying anti-rheumatic drugs (DMRDs). However, even though this approach provides fast relief, a financial concern comes up because conventional treatments require multiple administrations, possible hospitalization and the intervention of trained personnel, compromising the quality of life of patients (Rani et al., 2023). In this context, there is an urgent need for the development of novel, safe anti-inflammatory formulations with multiple mechanisms of action for the treatment of chronic inflammatory diseases due to the complexity of the related biological and molecular processes (Obluchinskaya et al., 2022).

* Corresponding author.
E-mail address: donatocosco@unicz.it (D. Cosco).

https://doi.org/10.1016/j.ijpharm.2024.124034
Received 24 January 2024; Received in revised form 7 March 2024; Accepted 20 March 2024
Available online 24 March 2024

Research is focusing on developing advanced therapies in the attempt to get around the risks of dose escalation-induced de-functionalization and therapeutic tolerance (Thorne et al., 2017). Several bioresponsive drug delivery systems have recently been used to address these issues and deliver drugs to treat chronic inflammatory diseases (Dou et al., 2020). For example, colloidal systems outperformed conventional formulations in terms of therapeutic compliance by increasing drug retention time at the site of action. The peculiar properties of nanoparticles, such as their mean sizes and large area-to-volume combined with the opportunity to functionalize their surfaces, enable them to interact with biological structures at both cellular and subcellular levels, opening up new avenues for personalized and targeted therapies (Zhang et al., 2012).

Brown algae might be a good alternative for the treatment of chronic disorders because it contains therapeutic components known as fucoidans (FU) —such as sulfated polysaccharides—which exert biological effects (Luthuli et al., 2019; Zayed and Ulber, 2019). These natural biomolecules have gained attention due to their potential anti-inflammatory, antioxidant, anticancer and immunomodulatory properties (Pradhan et al., 2020). FU were first discovered in 1913 and they have been used as a medicinal food supplement in Asia due to their pharmacological activities (Jin et al., 2021). Recent experimental studies focused on fucoidans obtained from *Fucus vesiculosus* and *Undaria pinnatifida* which belong to the *Fucales* and *Laminarales*, respectively (Bittkau et al., 2019). Interestingly, these FU have been observed to inhibit the activation of pathological pathways through a variety of cellular and molecular mechanisms. These include the inhibition of selectin-prostaglandin interaction, the suppression of the production of nitric oxide (Wang et al., 2021) along with the reduction of oxidative stress (Abdel-Daim et al., 2020), the selective inhibition of COX-2 (Pozharitskaya et al., 2020) and the down-regulation of the expression of mitogen-activated protein kinase p38, Akt, extracellular signal-regulated kinase and c-Jun N-terminal kinase (Park et al., 2011). Recently, Vaamonde-García et al, reported that FU have anti-oxidant and anti-inflammatory effects in chondrocytes, as well as having protective properties towards mitochondrial dysfunction (Vaamonde-García et al., 2021).

Sericin (SS) is another biopolymer characterized by several inherent biological properties. It's a globular water-soluble protein that, together with fibroin, constitutes the silk cocoon (Gagliardi et al., 2022). In recent years SS has been disposed of as industrial waste by the traditional silk industry, but it is making significant advances in regenerative medicine, tumor diagnostics, and materials science as a natural material In traditional medicine, natural SS was used as a cognitive enhancer and pain reliever for heart disease, atherosclerosis and metabolic disorders (Rahimpour et al., 2023). Indeed, the protein has been shown to suppress the inflammatory response by way of several mechanisms, including inhibition of the NF-κB and MAPK pathways, with a decreased secretion of pro-inflammatory cytokines (Aramwit et al., 2013; Song et al., 2016). Khampieng et al. demonstrated that SS-loaded alginate nanoparticles embedded in a hydrogel inhibited the carrageenan-induced inflammation and this effect was mainly due to the peculiar pharmacological properties of SS (Khampieng et al., 2015).

In the pursuit of more efficient treatments for chronic diseases such as inflammatory arthritis, the current study describes for the first time, to the best of the authors' knowledge, the potential application of nanoparticles made up of FU and SS as carriers of diclofenac sodium salt (DS), used as a model of nonsteroidal anti-inflammatory drug.

DS acts as a competitive and irreversible inhibitor of the prostatin synthase enzyme to treat inflammation and pain (Öztürk et al., 2020). Unlike many other NSAIDs, the most important advantage of this drug is that it exerts its therapeutic actions by a selective inhibition of COX-2 which is a key enzyme that can regulate the production of PGs. Moreover, multiple administrations of DS are required to maintain its therapeutic concentration because of its short biological half-life (2 h) and fast elimination rate (Altman et al., 2015).

These issues can be addressed through the encapsulation of the drug in the innovative hybrid formulation. Indeed, the association of the natural substances characterized by the aforementioned biological effects and the active compound might promote a decrease of its efficacious pharmacological concentration, potentially decreasing the risk of side effects, such as gastrointestinal, cardiac, hepatic and renal toxicity (McGettigan and Henry, 2013; Amanullah et al., 2022). The hybrid nanoparticles containing DS (DIFUCOSIN) were obtained through a simple and sustainable preparation process that does not include the use of homogenizers and their physico-chemical characterization and *in vitro* activity were investigated.

2. Materials and methods

2.1. Materials

Fucoidan (FU) from *Fucus Vescicolosus* (purity ≥ 95 %, ~70 kDa), commercial sericin (SS) from *Bombyx Mori*, diclofenac sodium salt (DS), sucrose, glucose, mannitol, mannose, sorbitol, 3-[4,5-dimethylthiazol-2-yl]-3,5-diphenyltetrazolium bromide salt, phosphate buffered saline (PBS) tablets, dimethyl sulfoxide, amphothericin B solution (250 μg/ml) Human chondrocytes (C28/I2) and Amicon® Ultracentrifugal filter units (MW 10 kDa), were all purchased from Sigma-Aldrich Co. (St. Louis, MO, USA). For the *in vitro* studies, DMEM (Dulbecco's Modified Eagle's Medium) with glutamine, trypsin, ethylene diamine tetraacetic acid (EDTA) (1 ×) solution, fetal bovine serum (FBS) and penicillin–streptomycin solution were obtained from Gibco (Life Technologies, Monza, Italy). The cellulose acetate membrane used for *in vitro* release studies (MW 50 kDa) was obtained from Spectrum Laboratories Inc. (Eindhoven, Netherlands). All other materials and solvents used in this investigation were of analytical grade (Carlo Erba, Milan, Italy).

2.2. Preparation of hybrid nanoparticles

The hybrid nanoparticles (hybrid NPs) made up of SS and FU were obtained using the desolvation method by adding an organic solvent to the aqueous polymer solution (Jahanban-Esfahlan et al., 2016; Kanoujia et al., 2016). In particular, various amounts of fucoidan (1–4 mg/ml) and a fixed quantity of sericin (3 mg/ml) were solubilized in 5 ml of an aqueous solution at room temperature. Acetone (4 ml) was added to the SS/FU solution at a rate of 1.0 ml/min under constant stirring at 600 rpm. The obtained dispersions were placed on a magnetic plate (600 rpm for 12 h) in order to favor the evaporation of the organic solvent. SS (3 mg/ml) or FU nanoparticles (4 mg/ml) were obtained using the same method by adding acetone (4 ml) to the aqueous polymer solution.

In addition, to obtain hybrid NPs containing DS, different amounts of drug (0.2–1 mg/ml) were solubilized in the polymer aqueous solution. Successively, the nanoparticles were purified by means of ultracentrifugation at 90 k × g for 60 min at 4 °C.

2.3. Physico-chemical characterization

Photon correlation spectroscopy (PCS) was used to evaluate the hydrodynamic diameter, size distribution and Zeta-potential of the hybrid NPs by using a Zetasizer Nano ZS (Malvern Panalytical Ltd., Spectris plc, England) and applying the third order cumulant correlation function. Each measurement was performed in triplicate on three different batches and reported as a function of the intensity (%) ± standard deviation. These parameters were also assessed as a function of temperature as previously described (Gagliardi et al., 2021).

A Transmission Electron Microscope (CM_{12} TEM, PHILIPS, The Netherlands) equipped with an OLYMPUS Megaview G_2 camera was used to investigate the morphology of hybrid NPs. The nanosystems were analyzed at 100 kV. A droplet of the sample was placed onto a carbon-coated copper screen. After drying, the sample was contrasted for two minutes with uranyl acetate and then washed with distilled

water.

2.4. Influence of pH and dispersing media

The influence of pH on the mean sizes, polydispersity index and zeta potential of the various hybrid formulations was evaluated by dispersing the samples in deionized water at different pH values (4.0, 7.0, 10.0), using 1 mol/l of NaOH or HCl.

Moreover, the formulations were incubated with the saline solution (NaCl 0.9 % w/v), the glucose solution (5 % w/v) and the PBS (0.01 M) in order to assess the influence of the dispersing media on the physical–chemical characteristics of the NPs as previously described (Ambrosio et al., 2023).

2.5. Lyophilization of nanosystems

The freeze-drying of the samples was performed as elsewhere described (Voci et al., 2022). Namely, different cryoprotectants (glucose, mannose, mannitol and sucrose) at concentrations of 5 and 10 % w/v were added to 1 ml of formulation in transparent pyrex vials and then frozen in liquid nitrogen for 2 min. Successively, the samples were placed in a freeze-drying chamber for 24 h (VirTis SP Scientific Sentry 2.0 apparatus with a vacuum pump B14 model, Carpanelli S.p.a., Bologna, Italy). The freeze-dried preparations were used after the reconstitution of the initial volume and analyzed by PCS.

The protective effect exerted by the various cryoprotectants was expressed as a redispersibility index (RDI) which was calculated according to the following equation:

$$RDI(\%) = D/D_0 \times 100 \quad (1)$$

where D is the mean diameter of the samples after the freeze-drying process, while D_0 refers to the mean diameters before the process. RDI values close or equal to 100 % identify samples that can be appropriately resuspended, while values above or below 100 % are typical of systems characterized by a non-ideal redispersibility (Voci et al., 2022).

2.6. Evaluation of the surface hydrophobicity and FT-IR analysis

The surface hydrophobicity of the hybrid NPs was investigated by means of the Rose bengal (RB) assay, as previously described with minor modifications (Doktorovova et al., 2012; Reboredo et al., 2021). Different concentration of NPs (6.33–1.616 mg/ml) were incubated under constant shaking for 30 min with 1 ml of an aqueous solution of RB (0.1 mg/ml). Successively, the samples were centrifuged for 30 min (4 °C, 90 k × g Beckman Ultracentrifuge Optima TL Beckman Coulter s.r. l., Milan, Italy) and the supernatant obtained at the end of the process analyzed at 548 nm using a Varioskan Lux microplate reader (Thermo Fischer Scientific, Waltham, Massachusetts, USA). For the evaluation of the surface hydrophobicity the Total Surface Area (TSA) of the hybrid NPs was calculated considering that the carriers were spherical in shape, monodispersed and having an average diameter equal to that determined by the PCS analyses, and by multiplying the surface (SA) of a single nanoparticle ($4\pi r^2$) for the total number of carriers occurring in each dilution (NT_{NPs}). This is shown in the following equation:

$$TSA = (SA_{NP}) \times (NT_{NPs}) \quad (2)$$

NT_{NPs} was obtained as the ratio between the weight of the samples in each dilution and the result obtained by multiplying the density of sericin fucoidan and zein (ρ = 10.11, 10.065, 1.41 g/cm^3, respectively, as calculated by picnometry) and the volume of a single NP ($4/3\pi r^3$):

$$NT_{NPs} = mNP/(\rho \times V_{NP}) \quad (3)$$

The partitioning quotient (PQ) of RB at each analyzed concentration was calculated as follows:

$$PQ = RBbound/RBunbound \quad (4)$$

where RB bound and RB unbound represent the amount of dye adsorbed onto the surfaces of the particles or dissociated from the carriers and found in the supernatant, respectively. The slope values obtained by plotting the TSA of the investigated nanosystems at a certain concentration versus the PQ of RB evidenced a linear correlation ($r^2 = 0.9970$) and represent the surface hydrophobicity of the samples. Generally, the higher the value of the slope obtained, the higher the hydrophobicity of the investigated sample (Khanal et al., 2016).

Moreover, a NicoletTM iS5 spectrometer coupled with an iD7 Attenuated Total Reflectance accessory (Thermo Fisher Scientific Inc., Waltham, MA, USA) was used to evaluate the vibrational spectra of SS, FU, DS, physical mixture, and freeze-dried NPs as empty systems or containing DS. A total of 64 acquisitions with a resolution of 4 cm^{-1} and a wavenumber range of 500–4000 cm^{-1} were used to obtain the FT-IR spectra. The OMNIC software was used to create the spectra analyses, version 9.12.1019. The reported findings represent an analysis of three separate experiments (Ambrosio et al., 2023).

2.7. Evaluation of the drug entrapment efficiency and release profiles

The amount of DS entrapped within the hybrid nanoparticles was determined by a suitable spectrophotometric method. In detail, the colloidal suspension containing the active compound was subjected to ultracentrifugation as previously described (section 2.2.) in order to separate the supernatant from the pellet. The supernatant was analyzed at a wavelength of 282 nm of the bioactive compound (Perkin Elmer Lambda 35) and the difference between the amount of the drug used initially during the sample preparation and that measured in the supernatant is the concentration of DS retained by the nanosystems. An empty colloidal formulation was used as blank.

The release profile of DS from hybrid NPs at various pHs (5 and 7.4) was assessed using the dialysis technique. Briefly, 1 ml of each formulation was put into a dialysis bag (cellulose acetate, cut-off 10 kDa, Spectrum Laboratories Inc. Netherlands), sealed with clips at both ends, and transferred to a beaker containing 200 ml of a constantly stirred PBS solution under sink conditions. (1) ml of release medium was removed and substituted with the same volume of fresh solution at various incubation times. The collected samples were successively analyzed by ~~a~~ the previously described spectrophotometric method. The ratio between the amount of the drug found in the release solutions (DS_{REL}) and that contained within the hybrid systems (DS_{LOAD}) was used to calculate the percentage of DS released, as reported below:

$$Release\% = DS_{REL}/DS_{LOAD} \times 100 \quad (5)$$

The results were described as the mean of three different experiments ± standard deviation.

Moreover, various mathematical models were used to analyze the percentage of cumulative drug release during the experiments. In particular, zero-order, first-order, Higuchi, Hixson-Crowell, and Korsmeyer-Peppas models were used to compare the obtained drug release kinetic profiles. The highest correlation coefficient (r^2) values indicate the most accurate and best-fitted kinetic models to describe the occurring drug release phenomena.

2.8. In vitro toxicity and anti-inflammatory activity

Human chondrocytes (C28/I2) were cultured as previously described (Cosco et al., 2016). The cytotoxicity of the aqueous solution of SS, FU and hybrid NPs was evaluated by MTT-testing. The cells were plated in 96-well culture plates (7×10^3 cellule/0.2 ml), treated with different concentrations of empty formulations (from 10, to 250 μg/ml of biomaterial) and incubated for 24, 48 and 72 h. Untreated cells were used as control. A microplate spectrophotometer (Thermo Scientific™

Varioskan™ LUX) was used to measure the cell viability at 540 nm with a reference wavelength of 690 nm. The cell viability was calculated according to the following equation after 3 h incubation with tetrazolium salts:

$$Cellviability\% = Abs_T Abs_C \times 100 \quad (6)$$

where Abs_T and Abs_C indicate the absorbance of treated and untreated cells, respectively. Each experiment was repeated three times, and cell viability values were calculated as the mean of each experiment ± standard deviation. The anti-inflammatory activity of empty nanoparticles, DS and DS-loaded hybrid NPs was investigated on C28/I2 cells by measuring specific markers such as IL-1β and IL-6. The cells were incubated with various concentrations of DS (free or nanoencapsulated) for 24 h before the addition of lipopolysaccharide (LPS) (100 ng/ml). IL-1β and IL-6 levels were measured at the end of the incubation period (24 h) using enzyme-linked immunoassorbent assay ELISA kits (Merck Millipore, Darmstadt, Germany) according to the manufacturer's instructions as previously reported (Cosco et al., 2016).

2.9. Cell uptake of rhodaminated nanoparticles by flow cytometry

Kinetics of intracellular accumulation of rhodaminated nanoparticles was evaluated by fluorescence-activated cell sorting (FACS) analysis as previously described (Fatma et al., 2016; Chiarella et al., 2020).

In detail, C28/I2 (2×10^5 cells/well) were treated with hybrid NPs prepared with rhodamine-DHPE (150 μg/ml) for various incubation times at 37 °C. Successively, cells were harvested by trypsinization, washed twice with ice-cold PBS and resuspended in 300 μl PBS for flow cytometry analysis. The fluorochrome was excited by means of a blue laser (488 nm) and 10,000 events were acquired on a BD FACscan™ II. The percentage of rhodamine-positive cells was determined by FlowJo software 8.8.6 (Becton Dickinson, Milan, Italy) using the histogram overlay method to show changes in expression profiles of each sample as compared to the untreated cells (Chiarella et al., 2020).

2.10. Statistical analysis

The statistical analysis of the various experiments was performed by ANOVA and the results confirmed by a Bonferroni t-test, with a p value of < 0.05 considered statistically significant.

3. Results and discussions

3.1. Physico-chemical features of hybrid nanoparticles

Nanosystems exhibit a wide range of physico-chemical properties, including size, shape, surface charge, and composition, for this reason a

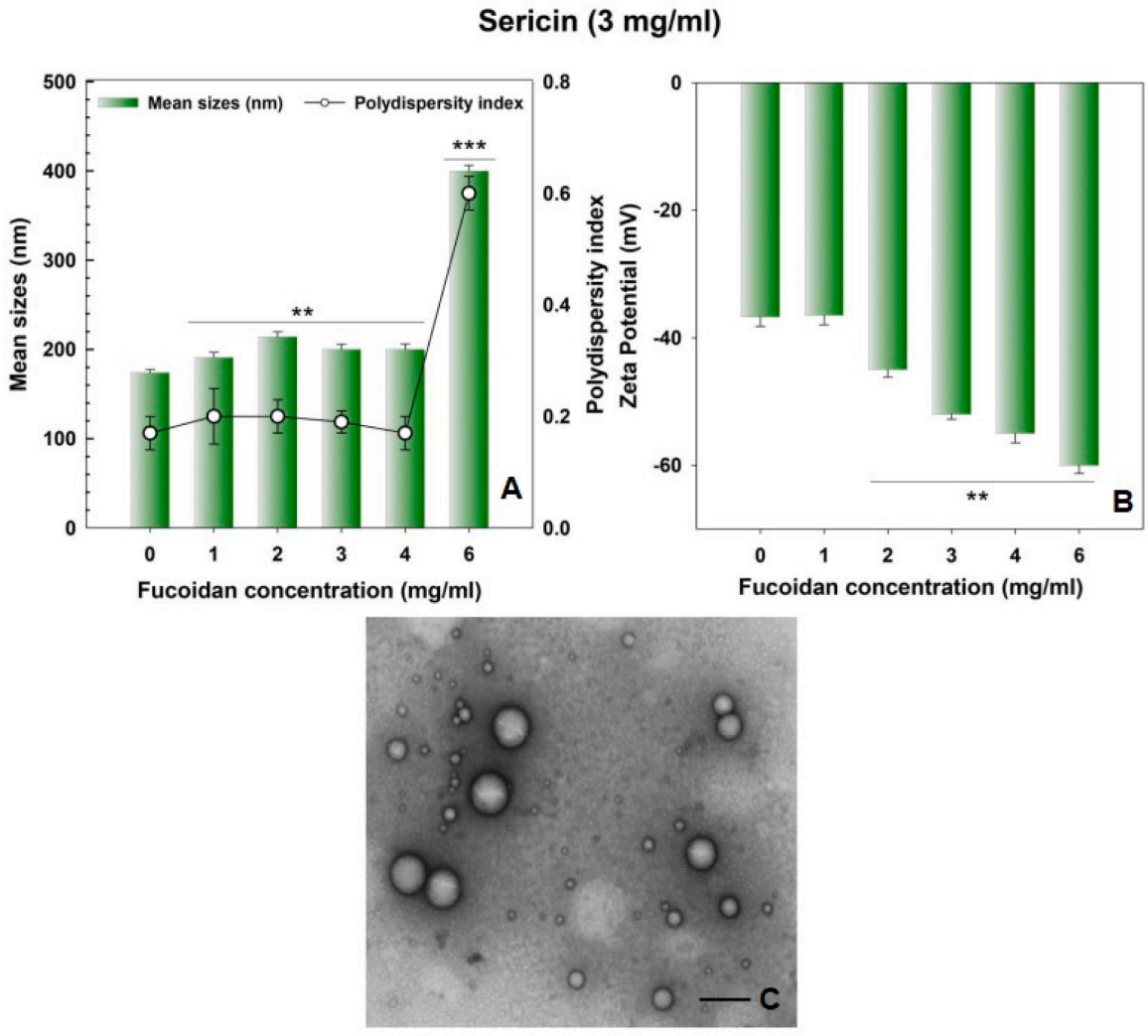

Fig. 1. (A) Mean sizes, polydispersity index and (B) surface charge of sericin nanoparticles (3 mg/ml) as a function of fucoidan concentration. (C) TEM micrograph of hybrid NPs prepared with 3 mg/ml of sericin and 4 mg/ml of fucoidan. Bar = 200 nm. $^{**}p < 0.01$, $^{***}p < 0.001$ vs. SS nanoparticles.

comprehensive understanding of these properties is essential in order to tailor these carriers for specific applications and ensure their stability under physiological conditions. As a result, in the first phase of the study, the impact of various amounts of FU on the formation of the sericin nanoparticles was investigated at a specific protein concentration (3 mg/ml), which was kept constant. This was because the systems obtained with this amount of biopolymer showed the best characteristics in terms of average diameter, polydispersity index (PDI), and zeta potential and no aggregates were observed during their preparation (Fig. S1). In particular, as shown in Fig. 1, variability in the dimensional values of the nanocarriers was obtained as a function of the amount of polysaccharide used.

The FU-free SS nanoparticles showed an average diameter of 170 nm, a PDI of ~ 0.12 and a negative surface charge. The addition of FU to the aqueous phase during the preparation step caused a slight increase in the mean diameter of the nanosystems up to a polysaccharide concentration of 4 mg/ml (Fig. 1). However, the use of 6 mg/ml of FU promoted the formation of macroaggregates and sediments. The PDI showed the same trend previously described but at a FU concentration of 3 and 4 mg/ml a significant decrease of the value was evident (Fig. 1). This phenomenon can be related to the high FU content which promoted an increase in the electrostatic repulsion between the colloidal particles, favoring the formation of a relatively stable colloidal structure, data in agreement with other studies based on hybrid FU nanosystems (Chen et al., 2018; Liu et al., 2020; Zhang et al., 2021). Moreover, the TEM technique was used to observe the morphology of the hybrid NPs and a well-defined, smooth, spherical structure was observed, confirming the PCS data previously discussed.

It has been widely demonstrated that proteins, when exposed to certain temperatures, can undergo structural rearrangements exposing new reactive sites (e.g. sulfhydryl groups and hydrophobic residues) capable of promoting various interactions between the polymer chains. Prolonged heat treatment, on the other hand, can favor the formation of aggregates as a result of the exposure of “sticky patches” composed of hydrophobic residues and cause a significant amount of unfolding structures affecting the stability of several formulations (Ma et al., 2020). For this reason, the various samples were also investigated as a function of the incubation temperature. As shown in Table 1, the FU-free formulation showed an increase of the mean sizes when the temperature was increased, a phenomenon probably due to protein rearrangement and a progressive destabilization of the colloidal structure. Contrarily, the addition of FU induced a slight increase in the mean diameter and the size distribution up to 40 °C, confirming the ability of the polysaccharide to prevent a temperature-dependent destabilization of the hybrid systems. However, it was interesting to note a significant variation of the aforementioned parameters at 50 °C with respect to the nanosystems incubated at 25 °C. In particular, the different formulations showed an increase in the surface charge (~-40 mV) with respect to the value obtained at room temperature. This phenomenon is probably due to the protein component which tends to rearrange itself at high temperatures, modulating the characteristics of the surface diffusion layer.

3.2. Influence of pH and dispersing media

Among the methods proposed for improving the therapeutic efficacy of NPs, the investigation of the physico-chemical characteristics of the formulations as a function of an external stimulus or/and the properties of the dispersant medium is a very fascinating approach. As can be seen in Fig. 2, the FU-free formulation showed a marked increase of the mean sizes in an acidic environment, probably due to the destabilization of the colloidal structure. The observation that incubation in an environment close to the isoelectric point of the protein (3.5) can promote adverse physical phenomena (a trend also confirmed by the zeta potential value close to 0), is in accordance with other experimental investigations (Hu et al., 2018) (Fig. 2). The addition of the polysaccharide avoided these adverse phenomena, probably as a consequence of the ionization of the negatively-charged sulfate groups of the polysaccharide which tend to interact more with the positively-charged groups of the protein, promoting a better stabilization of the colloidal structure (Fan et al., 2021). On the other hand, the presence of FU induced a slight increase of the PdI even though the mean diameter of the nanosystems was about of 200 nm (Fig. 2). These results are confirmed by many experimental studies which have demonstrated the ability of FU to stabilize nanoparticles made up of various materials such as chitosan, soy and zein, thanks to the high content of sulfate groups with a pKa value of around 2 which can easily be ionized when the pH range is between 2.0 and 8.0 (Coutinho et al., 2020; Ma et al., 2020). But the zeta potential of the various systems showed a clear increase at all the analyzed conditions, confirming a conformational rearrangement of the nanosystems (Fig. 2).

The effect of different dispersing media, such as saline solution (NaCl 0.9 % w/v), glucose solution (5 % w/v) and phosphate buffer (PBS 0.01 M) on the physico-chemical properties of a colloidal system is another

Table 1
Influence of temperature on the physico-chemical characteristics of the nanosystems based on sericin and fucoidan.

Sericin (mg/ml)	Fucoidan (mg/ml)	Temperature (°C)	Mean sizes (nm)	Polydispersity Index	Zeta Potential (mV)
3	–	25	174 ± 1	0.17 ± 0.03	−36 ± 1
3	–	30	177 ± 1	0.13 ± 0.02	−36 ± 1
3	–	40	234 ± 2***	0.24 ± 0.04*	−40 ± 1
3	–	50	286 ± 3***	0.30 ± 0.02***	–33 ± 1
3	1	25	198 ± 2	0.20 ± 0.02	−36 ± 1
3	1	30	210 ± 2	0.20 ± 0.02	−39 ± 1
3	1	40	220 ± 1*	0.21 ± 0.01	−38 ± 2
3	1	50	270 ± 2**	0.20 ± 0.04	−39 ± 1
3	2	25	205 ± 2	0.20 ± 0.01	−45 ± 1
3	2	30	211 ± 2	0.21 ± 0.01	−42 ± 1
3	2	40	222 ± 2*	0.20 ± 0.03	−42 ± 2
3	2	50	280 ± 3**	0.21 ± 0.06	−39 ± 1
3	3	25	200 ± 2	0.19 ± 0.01	−52 ± 2
3	3	30	209 ± 2	0.22 ± 0.01	−48 ± 2
3	3	40	230 ± 3*	0.22 ± 0.04	−43 ± 1*
3	3	50	307 ± 2***	0.25 ± 0.02	−40 ± 1*
3	4	25	210 ± 1	0.17 ± 0.02	−55 ± 2
3	4	30	220 ± 1*	0.21 ± 0.02	−50 ± 2
3	4	40	226 ± 5*	0.22 ± 0.05	−48 ± 1
3	4	50	306 ± 2**	0.22 ± 0.04	−45 ± 3*

*$p < 0.05$.
**$p < 0.01$.
***$p < 0.001$ vs. 25 °C.

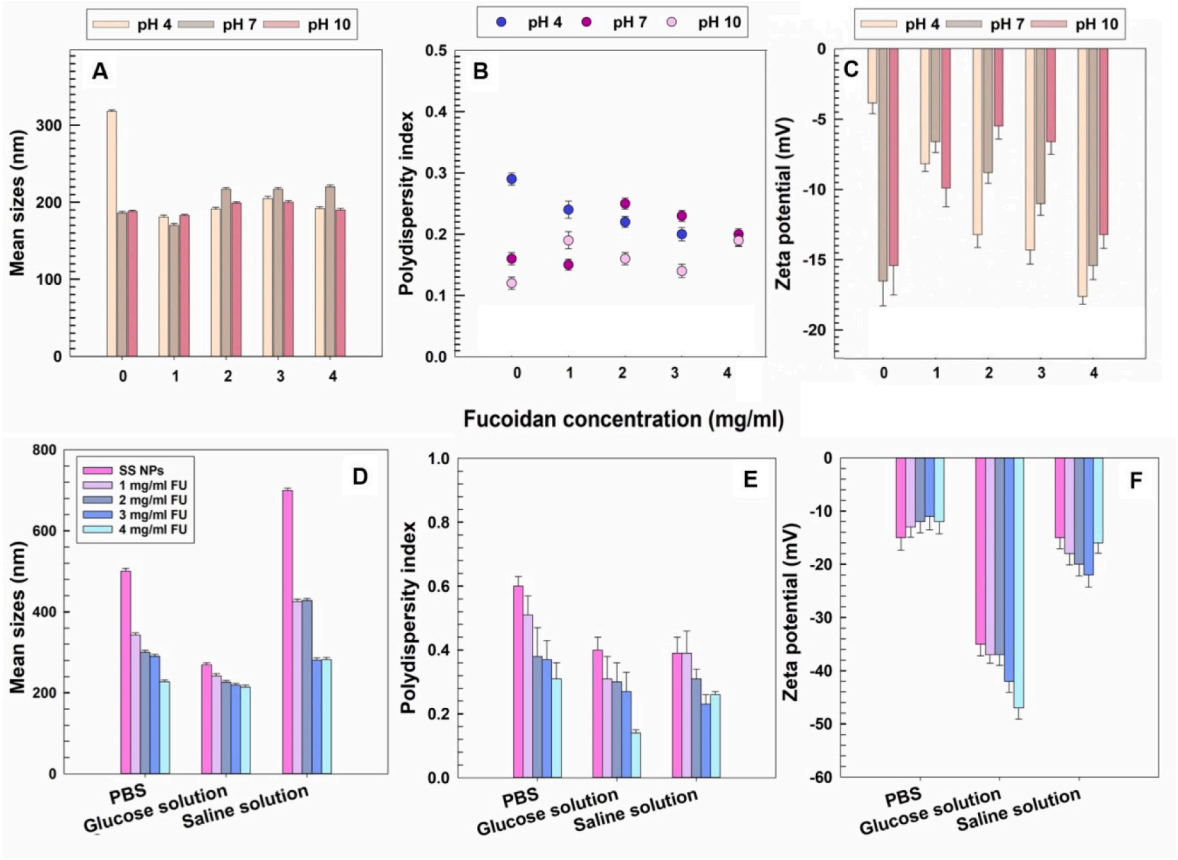

Fig. 2. Influence of pH and dispersing media on the average size (A, D), polydispersity index (B, E) and zeta potential (C, F) of the formulations made up of sericin (3 mg/ml) and different amounts of fucoidan.

important aspect to be evaluated during the steps of preformulation and before the *in vitro* and *in vivo* experiments. For this reason, the samples were prepared in the aforementioned media and their mean sizes, polydispersity index and zeta potential were evaluated by PCS. In detail, as can be seen in Fig. 2, the use of PBS promoted the formation of macroaggregates and a heterogeneous population. This phenomenon can be linked to the salting-out phenomenon; in fact, phosphate-salt-rich environments reduced the effectiveness of the electrostatic stabilization of the particles, resulting in the aggregation of the hydrophobic groups of the polymer in solution and favoring their precipitation. On the contrary, it was interesting to observe that the nanosystems prepared in 0.9 % NaCl and 5 % glucose solution preserved their mean diameter (around 200 nm) and showed. These results are very important because they demonstrate that the hybrid NPs prepared both in saline or in glucose solution could be systemically administered for various therapeutic purposes.

3.3. *Freeze-drying of hybrid nanoparticles*

Freeze-drying is a technique usually employed to achieve formulations characterized by long-term stability (Umerska et al., 2018). Freezing and/or drying a formulation can induce physical stress to the system. Generally, carbohydrates such as sucrose, trehalose and mannitol are the most commonly employed excipients to protect nanoparticles from these potential adverse phenomena and to prevent their aggregation (Mutukuri et al., 2021). In the first step of this investigation freeze-drying studies were performed on SS-NPs both with and without cryoprotectants in order to evaluate the appearance of aggregation phenomena due to the lyophilization process. As can be observed in Fig. 3, the freeze-dried nanoparticles without the cryoprotectant showed the best results in terms of average size (from 170 to 165) and polydispersity index (from 0.12 to 0.18) with a lesser negative surface charge though still around – 30 mV. These data were confirmed by the RDI which was close to 100 %, demonstrating the long-term storage stability of the systems (Fig. 3). Moreover, the cryoprotectants that allowed only a slight increase in the average diameter of the systems after redispersion were glucose and mannitol at 10 % w/v. However, in the current study, FU was used as a cryoprotectant and the hydrodynamic diameter, the PDI and the zeta potential of the samples were analyzed after their re-dispersion in water. As can be seen in Fig. 3, the freeze-dried NPs prepared with low concentrations of FU (1–2 mg/ml) showed a significant increase of the mean diameter (from about 200 nm to ~ 300 nm) and PDI (from 0.18 to 0.5). These data were confirmed by the redispersion index (RDI), demonstrating the inability of a low amount of the polysaccharide to bring about a suitable stabilization of the colloidal systems, as previously described by other experimental studies (Alkilany et al., 2014; Ball et al., 2017). On the other hand, the surface charge of the freeze-dried systems did not show significant variation.

Actually, it is interesting to note that the best results were obtained when higher concentrations of FU were used. In fact, the mean sizes and zeta potential of the lyophilized systems were very similar to those of the NPs before the freeze-drying process and the RDI was close to 100 % (Fig. 3). These data suggest that specific concentrations of FU are required in order to promote a protective, stabilizing effect on the SS nanoparticles and to avoid the necessity of adding other cryoprotectants to the formulation. Taking into consideration the data concerning the physico-chemical characterization of the nanosystems, the hybrid NPs prepared with 3 mg/mL of SS and 4 mg/mL of FU were chosen as a promising formulation to be used for additional experimental investigations because it is characterized by useful properties for drug delivery purposes.

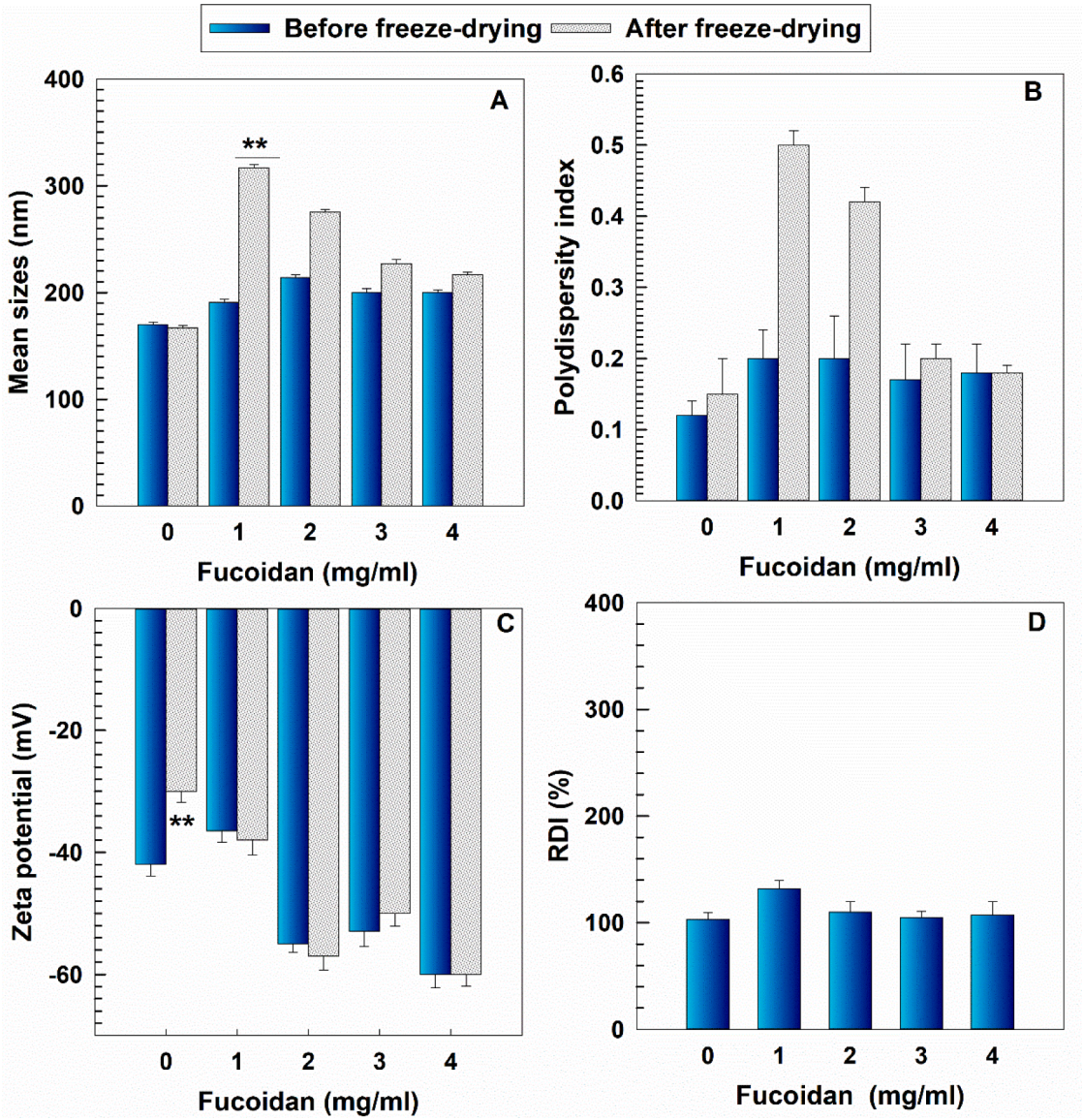

Fig. 3. (A) Mean diameter, (B) size distribution, (C) zeta potential, and (D) redispersibility index (RDI) of hybrid NPs prepared with 3 mg/ml of SS after a freeze-drying process as a function of the amount of FU. **p < 0.01 vs SS nanoparticles.

3.4. Physico-chemical characterization of DIFUCOSIN

The next step focused on the evaluation of the physico-chemical parameters of the hybrid nanoparticles as a function of various concentrations of DS, used as a model of anti-inflammatory hydrophilic drug. In detail, different amounts of the bioactive (0.2–1 mg/ml) were used to evaluate the ability of the hybrid systems to retain the compound. For this reason, the colloidal formulation required a new PCS characterization based on the amounts of DS initially used during the preparation phases of the samples.

As can be seen in Fig. 4, the addition of different concentrations of the drug did not have any significant effect on the mean diameter and polydispersity index of NPs with respect to the empty systems (Fig. 4). In fact, 0.2–0.8 mg/ml of DS allowed the formation of hybrid NPs with an average diameter of ~ 200 nm and a narrow size distribution (PDI= ~0.15). However, it was possible to observe that the concentration of 1 mg/ml of bioactive was the maximum that the nanosystems could stand because beyond that a destabilization of the colloidal structure with the formation of sediments and macroaggregates was promoted (data not shown). In addition, the zeta potential of the hybrid NPs was ~ -50 mV, demonstrating that DS had scarce impact on the surface charges of the nanosystems.

The ability of the polymeric matrix to retain the bioactive compound was investigated by means of spectrophotometric analysis. In detail, as shown in Fig. 4, the carriers were characterized by a high encapsulation rate of the molecule. In fact, a progressive increase in the amounts of DS retained by the hybrid nanoparticles with respect to the concentration of compound initially added can be observed. Specifically, an EE% of about 70 % was obtained using an initial drug amount of 0.8 mg/ml, while higher concentrations evidenced a decrease of the retained drug probably as a consequence of the adverse physical phenomena that occurred.

The release studies were performed in order to evaluate the leakage profiles of the bioactive over time under two physiological conditions, i.e. pHs 7 and 5, as the physiological and acidic environments, respectively. The drug release profiles from the hybrid NPs were very similar under both of the conditions, i.e. they were constant and protracted over time (Fig. 5). These results confirm the ability of fucoidan to keep the nanoparticles stable, promoting a great integration of the active compound into the nanosystems while permitting a constant and gradual release over time.

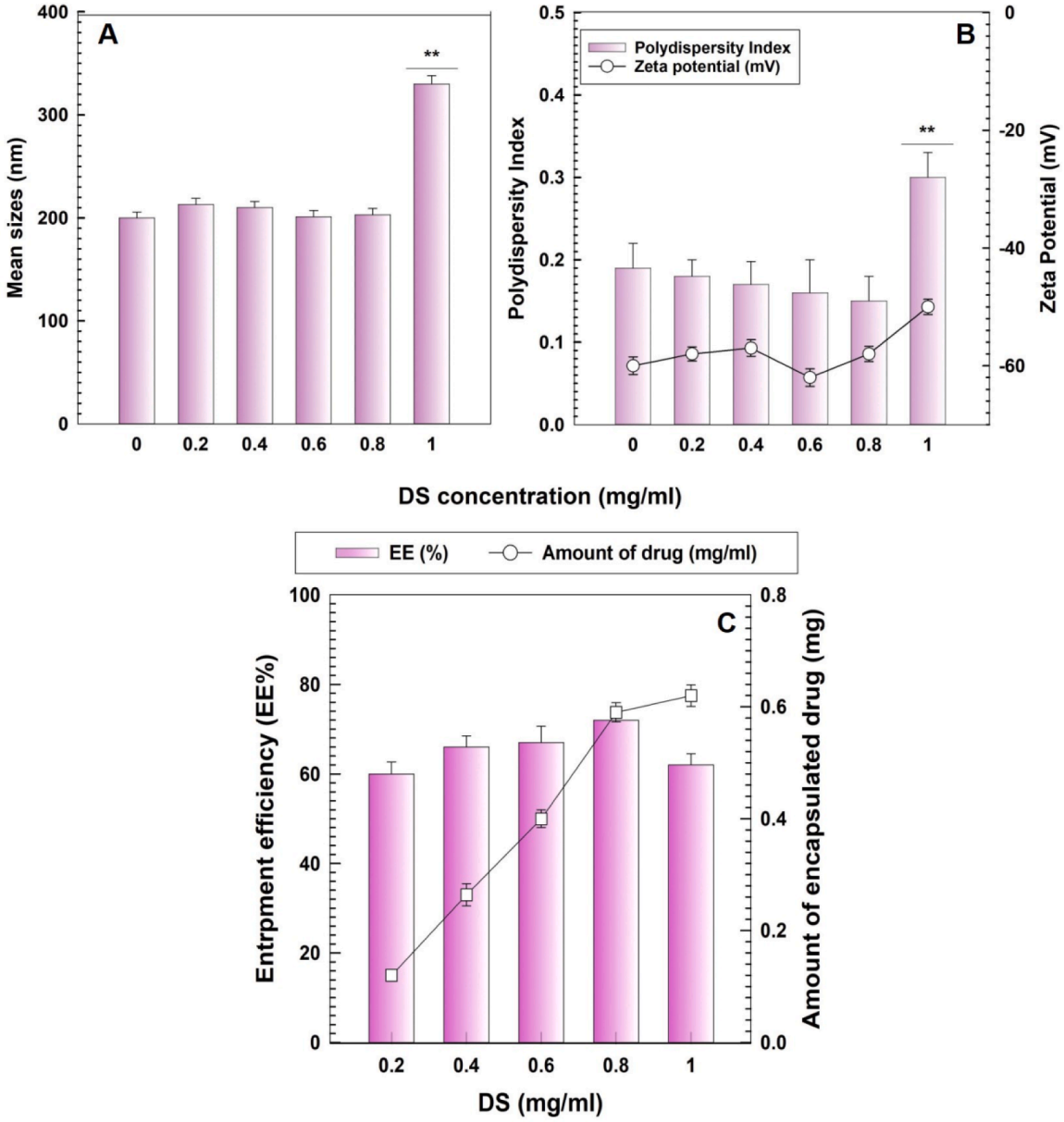

Fig. 4. Influence of various amounts of DS on the A) mean sizes, B) polydispersity index and surface charge, C) encapsulation efficiency (EE%) of hybrid nanoparticles made up of sericin (3 mg/ml) and fucoidan (4 mg/ml) as a function of the drug concentration initially added during the preparation of the samples. **$p < 0.01$ vs empty nanosystems.

In detail, the amount of encapsulated DS significantly influenced the drug leakage; in fact, it was interesting to note that the increase in the amount of the drug retained by the colloidal structure induced a milder and more prolonged release of the bioactive over time, confirming the great affinity of DS for the matrix. These results agree with previous experimental works based on hybrid systems made up of fucoidan and chitosan or sericin and zein, which showed that they efficiently retain hydrophilic compounds and are able to promote their controlled release (Elbi et al., 2017; Gagliardi et al., 2022).

In view of the previous results, the nanosystem formulation prepared with an initial DS concentration of 0.8 mg/ml was selected as the ideal formulation to be used for additional experiments. The release profile of DS from this system was analyzed using various mathematical models such as zero-order, first-order, Higuchi, Hixson-Crowell, and Korsmeyer-Peppas in order to better understand the mechanisms governing the drug leakage from the nanosystems (Table 2).

The correlation coefficient (r^2) was used as a fitness criterion, which provided valuable information regarding the fitting quality. The results showed that Higuchi was the best-fitting model for DS release under both pH conditions, evidencing that the principal phenomenon involved in drug leakage is the diffusion process based on Fick's law, which is square root-time dependent.

3.5. Evaluation of FT-IR spectra and surface properties of hybrid nanoparticles

The surface properties of the hybrid NPs were investigated using the Rose Bengal assay. For this experiment, zein NPs were used as control because the vegetal protein is a well-known model of a hydrophobic raw material. Fig. 6 shows the variation of the surface hydrophobicity of the investigated nanosystems as a function of the biomaterial used in their preparation. In detail, SS and FU-NPs evidenced a greater hydrophilic character with respect to zein nanoparticles due to their composition, although it was interesting to observe the influence exerted by the

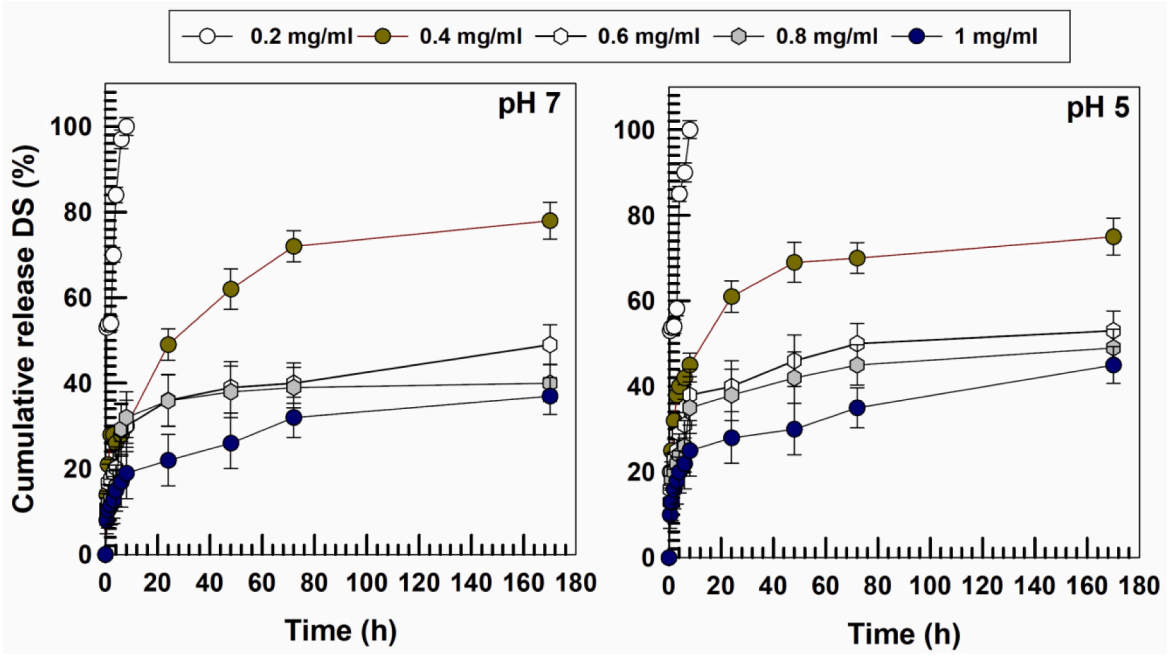

Fig. 5. Release profiles of DS from hybrid nanoparticles in physiological (pH 7) and acidic (pH 5) environments as a function of the amount of encapsulated drug and the incubation time. The analysis was performed at 37 °C. Values are the result of three experiments ± standard deviation.

Table 2
Correlation coefficient (r^2) of release kinetics of DS from hybrid NPs according to various mathematical models.

Release medium	Zero-order	First-order	Higuchi	Korsmeyer-Peppas	Hixson-Crowel
Aqueous solution (pH 5)	0.6754	0.7636	0.9803	0.8704	0.7348
PBS (pH 7)	0.7048	0.7626	0.9905	0.8618	0.7436

polysaccharide against the surface properties of the empty- and DIFUCOSIN NPs. Indeed, it is clear that fucoidan is the principal modulator of relative surface hydrophobicity, demonstrating a two-fold increase of this parameter when compared to SS NPs (Fig. 6).

These results are surprising considering the water-soluble character of the selected biomaterials. In any case, this result is consistent with recent findings reported for hybrid nanosystems made up of ovalbumin and fucoidan (Sun et al., 2023). More specifically, it was demonstrated that fucoidan can confer a certain degree of hydrophobicity to the nanostructures by replacing the lipophilic residues of globular proteins, such as ovalbumin and sericin, keeping them buried in their inner core (Dautel and Champion, 2020; Duan et al., 2023).

Contrarily, the addition of the active compound did not evidence any significant variation of the surface properties of the nanosystems with

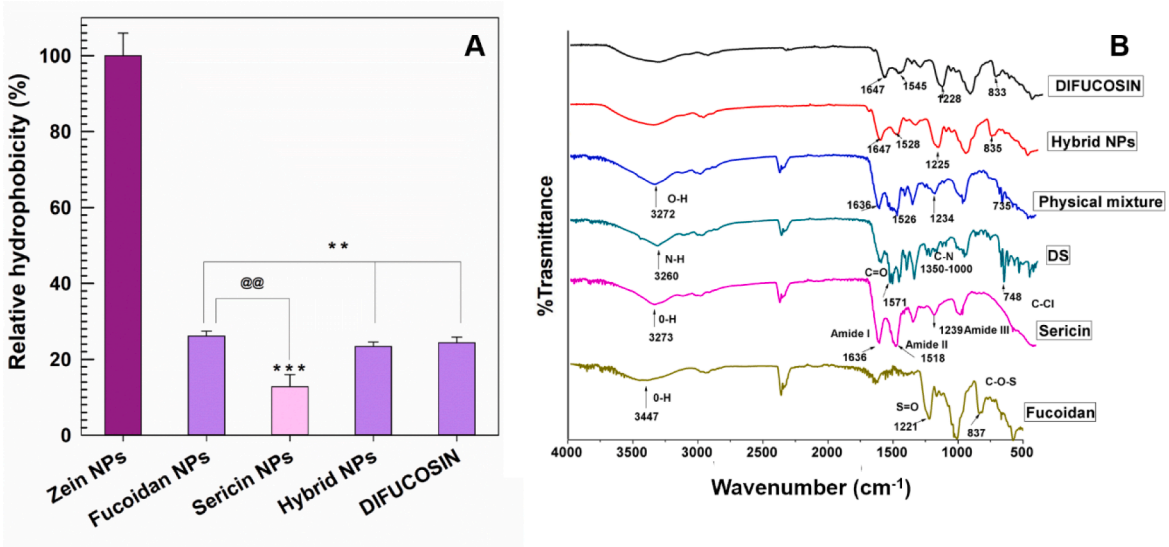

Fig. 6. (A) Surface hydrophobicity of FU NPs (4 mg/ml), SS NPs (3 mg/ml), hybrid NPs made up of fucoidan (4 mg/ml) and sericin (3 mg/ml) and DIFUCOSIN NPs. $^{**}p < 0.001$ and $^{***}p < 0.0001$ with respect to zein NPs used as control; $^{@@}p < 0.001$ Fucoidan NPs vs Sericin NPs. The results are reported as the mean of three different experiments ± the standard deviation. Zein NPs were used as control. (B) FT-IR spectra of the various components of the formulations, their physical mixture, empty and DIFUCOSIN NPs.

respect to the empty hybrid NPs, demonstrating that the active compound doesn't significantly modify the physico-chemical properties of the colloidal carriers (Fig. 6).

In addition, the FT-IR spectra of the various components of the nanosystems and DS are shown in Fig. 6. In particular, the FT-IR profile of the DS evidenced the following characteristic peaks: 3260 cm^{-1} (due to N–H stretching vibrations), 1571 cm^{-1} (C = O carboxylate ion stretching), 748 cm^{-1} (due to C-Cl stretching) and peaks between 1000 cm^{-1} and 1350 cm^{-1}, corresponding to the stretching of the C-N group (Öztürk et al., 2020; Akbari et al., 2022).

The FU spectrum showed a broad band at 3447 cm^{-1} (O–H group stretching), a peak at around 1221 cm^{-1} (S = O stretching) and another peak at 837 cm^{-1} (C-O-S bending vibration) which have been attributed to the existence of the considerable amount of sulfate ester groups in the polysaccharide (Q. Liu et al., 2020).

Additionally, the characteristic bands of SS were observed at 3273 cm^{-1} (O–H group stretching); the amide I peak at 1636 cm^{-1} which was attributed to C = O stretching of the carbonyl group, the peak at 1518 cm^{-1} attributed to N–H bending and C-N stretching vibrations (amide II), and the amide III peak at 1239 cm^{-1} due to the interactions of C-N stretching and N–H bending (Radu et al., 2021; Zhu et al., 2022).

As can be seen in Fig. 6, in the hybrid NPs the O–H vibration absorption band of FU at 3447 cm^{-1} shifted towards 3292 cm^{-1}; moreover, the peaks of amides I and II of the protein underwent a further shift from 1636 to 1647 and from 1518 to 1528 cm^{-1}, respectively. These results demonstrated that the predominant interactions of the nanosystems are the electrostatic and hydrogen bonds between the protein and the polysaccharide.

Interestingly, in the spectrum of DIFUCOSIN nanoparticles, the characteristic absorption bands of the active compound decrease or even disappear and this is a clear indication of the overlapping of the peculiar peaks of the DS with those of the polymeric matrix. This trend is divergent from that obtained in the case of the physical mixture in which the peculiar peaks of the drug can be observed, even though in a less marked way. The changes in FT-IR signals indicated that the drug had been effectively encapsulated within the colloidal particles.

3.6. Cytotoxicity of hybrid NPs

The intrinsic toxicity of hybrid NPs has been evaluated on human C28/I2 chondrocytes since diverse studies revealed the anti-inflammatory activity of DS on models of C28/I2-derived pathological cartilage (Chang et al., 2021). As can be seen in Fig. S2, both FU and SS showed a certain cytotoxicity only after 72 h incubation at the highest concentrations. In particular, the polymers promoted a decrease in the cell viability of 20 % at a concentration of 250 μg/ml, confirming the low level of toxicity of these biomaterials (Fig. S2). These results are consistent with several studies focused on SS which described the very low toxicity of protein-based nanoparticles when large amounts of the biopolymer were used (1000 μg/ml) (Gagliardi et al., 2022). But even FU-based nanosystems have shown mild toxicity on various cell lines, including THP-1, K562, HS-Sultan, NB4, BCBL-1, TY-1, HL-60 and U937 when concentrations of the polysaccharide up to 200 μg/ml were employed (Ahmad et al., 2021). The nanoformulations reduced cell viability at polymer concentrations greater than 100 μg/ml and incubation times over 48 h (Fig. S2). These results demonstrated the biocompatibility of the hybrid carriers, although the toxic concentrations herein described were never reached in the following experiments.

Additionally, the kinetics of the intracellular accumulation of rhodaminated nanoparticles were evaluated by cytofluorometry. C28/I2 cells were cultured in the presence of 150 μg/ml empty nanocarriers for 30, 60, 120, 240 and 360 min and then intracellular fluorescence was measured (Fig. 7). FACS analysis showed a significant cell uptake of the fluorescent nanoparticles following 1 h incubation, and a subsequent progressive increase of the signal after 2 and 4 h. The fluorescence signal appeared to be stable when the cells were incubated with the rhodaminated hybrid nanoparticles for 6 h. In addition, the average of the intensity of red fluorescence in C28/I2 cells gradually increased over

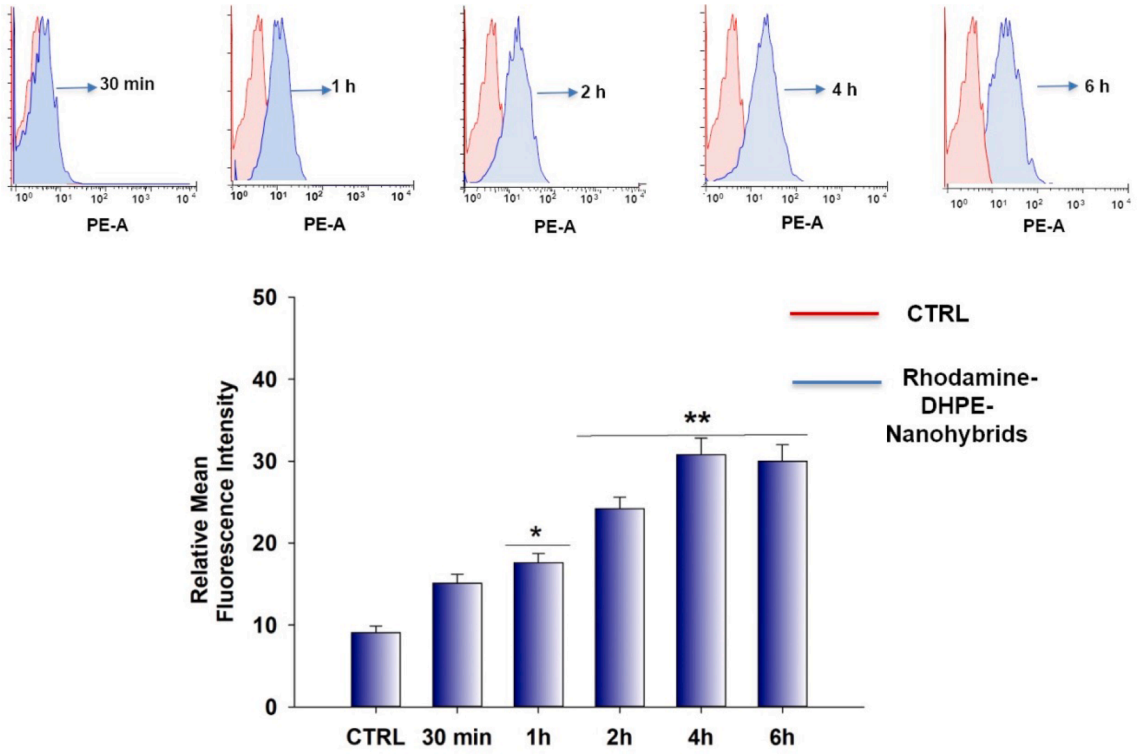

Fig. 7. Cytometric flow analysis of C28/I2 cells treated with rhodamine-DHPE-labelled hybrid nanoparticles (upper panel). Relative mean fluorescence intensity expressed as fold of increase with respect to untreated cells (lower panel). The results represent the mean ± SD of three independent experiments. *$p < 0.05$ **$p < 0.01$ with respect to CTRL.

time, confirming a time-dependent cell uptake of fluorescent nanosystems (Fig. 7).

Successively, the anti-inflammatory activity of DS and DIFUCOSIN was evaluated as a function of the drug concentration. In particular, C28/I2 cells were pre-incubated with the various formulations for 24 h and then treated with LPS. Several studies in literature reported that FU and SS are characterized by a noteworthy *in vitro* and *in vivo* anti-inflammatory properties, and thus they can be employed in various diseases such as cancer and pathogenic infections (Aramwit et al., 2013; Obluchinskaya et al., 2022; Wang et al., 2023).

Many inflammatory lesions are caused by changes in the production or function of cytokines such as IL-6 and IL-1β. Inflammatory stimuli, such as that exerted by LPS, induce great cytokine production by the macrophages, which is then amplified by autocrine and paracrine pathways that are able to increase the severity of the immune response and the inflammation that follows. For this reason, the inhibition of cytokine expression or function is an important mechanism in the regulation of inflammation.

As shown in Fig. 8, even though the expression of IL-6 was already elevated due to the inherent characteristic of C28/I2 which constitutively expressed large quantities of this marker, the levels of pro-inflammatory cytokines increased with LPS (Kloesch et al., 2011). It can be observed that all the formulations at both concentrations decreased the levels of the interleukines. It is well-known that DS exerts anti-inflammatory activities, but its entrapment within hybrid nanoparticles significantly enhanced the obtained effect with respect to that of the free drug.

It is interesting to note that the empty formulation induced a significant decrease in the levels of the two inflammation markers. This phenomenon is probably related to the inherent properties of both polymers that act as strong inflammation inhibitors by down-regulating the production of pro-inflammatory cytokines. In fact, according to several experimental studies, FU can inhibit the expression of COX-2 in a dose- and time-dependent manner in articular rabbit chondrocytes (Garcia et al., 2019; Vaamonde-Garcia et al., 2021). Additionally, Obluchinskaya et al. demonstrated that a FU-based cream can decrease the carrageenan-induced edema in rats after topical application in a dose-dependent manner and in a similar way to that of a diclofenac gel (Obluchinskaya et al., 2022). Similarly, Sun et al., described that SS inhibited LPS-induced inflammation through the NF-κB pathway (which is a key regulator of inflammation), decreases the downstream inflammatory cytokine expression (Aramwit et al., 2013; Sun et al., 2022). This finding suggests that the proposed hybrid nanoparticles could be helpful in the treatment of various inflammatory diseases.

4. Conclusions

NSAIDs are the most commonly prescribed drugs due to their efficacy and ample availability, accounting for 5 % of all drugs prescribed worldwide (Panchal and Sabina, 2023). But despite their numerous therapeutic benefits, NSAIDs have serious side effects, being responsible for over 30 % of hospitalizations due to overdosage. Indeed, several pharmaco-epidemiological studies have shown an uncontrolled increase in the use of NSAIDs in recent years, which could be one of the reasons for its emerging toxicity (Moore et al., 2019). The use of hybrid nanoparticles made up of natural polymers for the management of chronic inflammatory diseases represents an exciting frontier in medical and pharmaceutical research. These innovative approaches have the potential to address multi-faceted criticism related to this condition, ranging from inflammation control and cartilage protection to drug delivery and joint lubrification. As research progresses, they could potentially offer new strategies for enhancing the quality of life of patients affected by a wide range of diseases. Indeed, materials having multiple-responsive characteristics are a breakthrough in carrier performance thanks to both the specific peculiar and common advantages of each individual component. Nonetheless, few clinical trials have been completed to date, most likely due to a lack of comparative research between various fucoidans and specific experimental disease models.

In this investigation, for the first time to the best of the authors' knowledge, SS and FU have been associated in order to obtain colloidal systems able to retain DS with the aim of exploiting the inherent anti-inflammatory properties of the biomaterials and preserving the pharmacological effect of the active compound. The obtained hybrid nanosystems were characterized by a significant physical stability, a prolonged drug leakage over the time and they demonstrated a noteworthy decrease of pro-inflammatory markers.

Despite the promising results described in this investigation, it is important to emphasize that this is a preliminary study and additional research is required to better understand the mechanisms involved in the anti-inflammatory activity of DIFUCOSIN, its safety, *in vivo* biodistribution and the real efficacy as a novel nanomedicine for the treatment of inflammatory diseases.

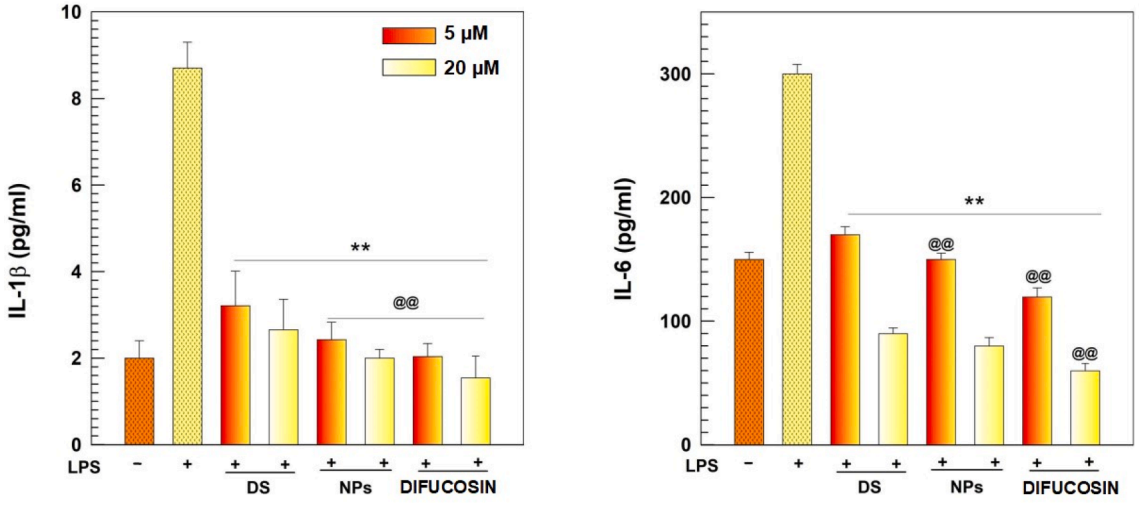

Fig. 8. Anti-inflammatory activity of DS as free drug or encapsulated within hybrid NPs assayed in C28/I2 cell cultures. The cells were incubated for 24 h with various concentrations of the active compound (5 and 20 μM) and then treated with LPS (200 ng/ml) for 24 h. At the end of the incubation time, IL-1β and IL-6 were quantified utilizing suitable ELISA kits. Values are the average of three different experiments ± standard deviation. $^{**}p < 0.01$ with respect to LPS and $^{@@}p < 0.01$ with respect to DS.

Funding statement

This research was funded by a grant from the Italian Ministry of University and Research (PRIN2022_PNRR, prot. n. P202242HYK).

Open access funding provided by "Università degli Studi Magna Graecia di Catanzaro" within the CRUI-CARE Agreement.

CRediT authorship contribution statement

Agnese Gagliardi: Writing – review & editing, Writing – original draft, Software, Investigation, Formal analysis, Conceptualization. **Emanuela Chiarella:** Writing – review & editing, Software, Methodology, Investigation, Formal analysis. **Silvia Voci:** Validation, Software, Formal analysis, Data curation. **Nicola Ambrosio:** Visualization, Software, Data curation. **Marilena Celano:** Writing – review & editing, Validation, Formal analysis, Data curation. **Maria Cristina Salvatici:** Validation, Software, Methodology, Investigation. **Donato Cosco:** Writing – review & editing, Validation, Supervision, Resources, Project administration, Funding acquisition, Conceptualization.

Declaration of competing interest

The authors declare that they have no known competing financial interests or personal relationships that could have appeared to influence the work reported in this paper.

Data availability

Data will be made available on request.

Acknowledgments

The authors are grateful to Lynn Whitted for her language revision of this article.

Appendix A. Supplementary data

Supplementary data to this article can be found online at https://doi.org/10.1016/j.ijpharm.2024.124034.

References

Abdel-Daim, M.M., Abushouk, A.I., Bahbah, E.I., Bungău, S.G., Alyousif, M.S., Aleya, L., Alkahtani, S., 2020. Fucoidan protects against subacute diazinon-induced oxidative damage in cardiac, hepatic, and renal tissues. Environ. Sci. Pollut. Res. 27, 11554–11564. https://doi.org/10.1007/s11356-020-07711-w.

Ahmad, T., Eapen, M.S., Ishaq, M., Park, A.Y., Karpiniec, S.S., Stringer, D.N., Sohal, S.S., Fitton, J.H., Guven, N., Caruso, V., 2021. Anti-inflammatory activity of fucoidan extracts in vitro. Mar. Drugs 19, 702. https://doi.org/10.3390/md19120702.

Akbari, J., Saeedi, M., Morteza-Semnani, K., Hashemi, S.M.H., Babaei, A., Eghbali, M., Mohammadi, M., Rostamkalaei, S.S., Asare-Addo, K., Nokhodchi, A., 2022. Innovative topical niosomal gel formulation containing diclofenac sodium (niofenac). J. Drug Target. 30, 108–117. https://doi.org/10.1080/1061186X.2021.1941060.

Alkilany, A.M., Abulateefeh, S.R., Mills, K.K., Bani Yaseen, A.I., Hamaly, M.A., Alkhatib, H.S., Aiedeh, K.M., Stone, J.W., 2014. Colloidal stability of citrate and mercaptoacetic acid capped gold nanoparticles upon lyophilization: effect of capping ligand attachment and type of cryoprotectants. Langmuir 30, 13799–13808. https://doi.org/10.1021/la504000v.

Altman, R., Bosch, B., Brune, K., Patrignani, P., Young, C., 2015. Advances in NSAID development: evolution of diclofenac products using pharmaceutical technology. Drugs 75, 859–877. https://doi.org/10.1007/s40265-015-0392-z.

Amanullah, A., Upadhyay, A., Dhiman, R., Singh, S., Kumar, A., Ahirwar, D.K., Gutti, R. K., Mishra, A., 2022. Development and challenges of diclofenac-based novel therapeutics: targeting cancer and complex diseases. Cancers (basel). 14, 4385. https://doi.org/10.3390/cancers14184385.

Ambrosio, N., Gagliardi, A., Voci, S., Salvatici, M.C., Fresta, M., Cosco, D., 2023. Strategies of stabilization of zein nanoparticles containing doxorubicin hydrochloride. Int. J. Biol. Macromol. 243, 125222 https://doi.org/10.1016/j.ijbiomac.2023.125222.

Aramwit, P., Towiwat, P., Srichana, T., 2013. Anti-inflammatory potential of silk sericin. Nat. Prod. Commun. 8, 1934578X1300800424 https://doi.org/10.1177/1934578X1300800424.

Ball, R.L., Bajaj, P., Whitehead, K.A., 2017. Achieving long-term stability of lipid nanoparticles: examining the effect of pH, temperature, and lyophilization. Int. J. Nanomedicine 12, 305. https://doi.org/10.2147/IJN.S123062.

Bittkau, K.S., Dörschmann, P., Blümel, M., Tasdemir, D., Roider, J., Klettner, A., Alban, S., 2019. Comparison of the effects of fucoidans on the cell viability of tumor and non-tumor cell lines. Mar. Drugs 17, 441. https://doi.org/10.3390/md17080441.

Chang, M.C., Chiang, P.F., Kuo, Y.J., Peng, C.L., Chen, K.Y., Chiang, Y.C., 2021. Hyaluronan-loaded liposomal dexamethasone–diclofenac nanoparticles for local osteoarthritis treatment. Int. J. Mol. Sci. 22, 665. https://doi.org/10.3390/ijms22020665.

Chapman, L.S., Backhouse, M., Bearne, L., Cherry, L., Cleary, G., Davey, J., Ferguson, R., Grieve, A., Helliwell, P., Lomax, A., McKeeman, H., Rawlings, A., Rees, R., Rooney, R., Ryan, S., Sanders, L., Siddle, H.J., Varley, S., Warburton, L., Woodburn, J., Roddy, E., 2022. Management of foot health in people with inflammatory arthritis: British Society for Rheumatology guideline scope. Rheumatology (Oxford) 61, 3907–3911. https://doi.org/10.1093/rheumatology/keac340.

Chen, C.H., Lin, Y.-S., Wu, S.J., Mi, F.L., 2018. Mutlifunctional nanoparticles prepared from arginine-modified chitosan and thiolated fucoidan for oral delivery of hydrophobic and hydrophilic drugs. Carbohydr. Polym. 193, 163–172. https://doi.org/10.1016/j.carbpol.2018.03.080.

Chiarella, E., Lombardo, N., Lobello, N., Piazzetta, G.L., Morrone, H.L., Mesuraca, M., Bond, H.M., 2020. Deficit in adipose differentiation in mesenchymal stem cells derived from chronic rhinosinusitis nasal polyps compared to nasal mucosal tissue. Int. J. Mol. Sci. 21 https://doi.org/10.3390/ijms21239214.

Cosco, D., Failla, P., Costa, N., Pullano, S., Fiorillo, A., Mollace, V., Fresta, M., Paolino, D., 2016. Rutin-loaded chitosan microspheres: characterization and evaluation of the anti-inflammatory activity. Carbohydr. Polym. 152, 583–591. https://doi.org/10.1016/j.carbpol.2016.06.039.

Coutinho, A.J., Costa Lima, S.A., Afonso, C.M.M., Reis, S., 2020. Mucoadhesive and pH responsive fucoidan-chitosan nanoparticles for the oral delivery of methotrexate. Int. J. Biol. Macromol. 158, 180–188. https://doi.org/10.1016/j.ijbiomac.2020.04.233.

Dautel, D.R., Champion, J.A., 2020. Protein vesicles self-assembled from functional globular proteins with different charge and size. Biomacromolecules 22, 116–125. https://doi.org/10.1021/acs.biomac.0c00671.

Doktorovova, S., Shegokar, R., Martins-Lopes, P., Silva, A.M., Lopes, C.M., Müller, R.H., Souto, E.B., 2012. Modified rose Bengal assay for surface hydrophobicity evaluation of cationic solid lipid nanoparticles (cSLN). Eur. J. Pharm. Sci. off. J. Eur. Fed. Pharm. Sci. 45, 606–612. https://doi.org/10.1016/j.ejps.2011.12.016.

Dou, Y., Li, C., Li, L., Guo, J., Zhang, J., 2020. Bioresponsive drug delivery systems for the treatment of inflammatory diseases. J. Control. Release 327, 641–666. https://doi.org/10.1016/j.jconrel.2020.09.008.

Duan, W., Chen, L., Liu, F., Li, X., Wu, Y., Cheng, L., Liu, J., Ai, C., Huang, Q., Zhou, Y., 2023. The properties and formation mechanism of ovalbumin-fucoidan complex. Int. J. Biol. Macromol. 241, 124644 https://doi.org/10.1016/j.ijbiomac.2023.124644.

Elbi, S., Nimal, T.R., Rajan, V.K., Baranwal, G., Biswas, R., Jayakumar, R., Sathianarayanan, S., 2017. Fucoidan coated ciprofloxacin loaded chitosan nanoparticles for the treatment of intracellular and biofilm infections of Salmonella. Colloids Surfaces B Biointerfaces 160, 40–47. https://doi.org/10.1016/j.colsurfb.2017.09.003.

Fan, L., Lu, Y., Ouyang, X., Ling, J., 2021. Development and characterization of soybean protein isolate and fucoidan nanoparticles for curcumin encapsulation. Int. J. Biol. Macromol. 169, 194–205. https://doi.org/10.1016/j.ijbiomac.2020.12.086.

Fatma, S., Talegaonkar, S., Iqbal, Z., Panda, A.K., Negi, L.M., Goswami, D.G., Tariq, M., 2016. Novel flavonoid-based biodegradable nanoparticles for effective oral delivery of etoposide by P-glycoprotein modulation: an in vitro, ex vivo and in vivo investigations. Drug Deliv. 23, 500–511. https://doi.org/10.3109/10717544.2014.923956.

Gagliardi, A., Voci, S., Bonacci, S., Iriti, G., Procopio, A., Fresta, M., Cosco, D., 2021. SCLAREIN (SCLAREol contained in zeIN) nanoparticles: development and characterization of an innovative natural nanoformulation. Int. J. Biol. Macromol. 193, 713–720. https://doi.org/10.1016/j.ijbiomac.2021.10.184.

Gagliardi, A., Ambrosio, N., Voci, S., Salvatici, M.C., Fresta, M., Cosco, D., 2022. Easy preparation, characterization and cytotoxic investigation of 5-Fluorouracil-loaded zein/sericin nanoblends. J. Mol. Liq. 366, 120344 https://doi.org/10.1016/j.molliq.2022.120344.

Garcia, C.V., Lamas-Vazquez, M., Blanco, F., Dominguez, H., Meijide-Failde, R., 2019. Impact of different fucoidans on pathological pathways activated in osteoarthritic articular cells. Osteoarthr. Cartil. 27, S147–S148. https://doi.org/10.1016/j.joca.2019.02.214.

Hu, D., Li, T., Xu, Z., Liu, D., Yang, M., Zhu, L., 2018. Self-stabilized silk sericin-based nanoparticles: in vivo biocompatibility and reduced doxorubicin-induced toxicity. Acta Biomater. 74, 385–396. https://doi.org/10.1016/j.actbio.2018.05.024.

Jahanban-Esfahlan, A., Dastmalchi, S., Davaran, S., 2016. A simple improved desolvation method for the rapid preparation of albumin nanoparticles. Int. J. Biol. Macromol. 91, 703–709. https://doi.org/10.1016/j.ijbiomac.2016.05.032.

Jin, J.O., Chauhan, P.S., Arukha, A.P., Chavda, V., Dubey, A., Yadav, D., 2021. The therapeutic potential of the anticancer activity of fucoidan: current advances and hurdles. Mar. Drugs 19, 265. https://doi.org/10.3390/md19050265.

Kanoujia, J., Singh, M., Singh, P., Saraf, S.A., 2016. Novel genipin crosslinked atorvastatin loaded sericin nanoparticles for their enhanced antihyperlipidemic activity. Mater. Sci. Eng. C. Mater. Biol. Appl. 69, 967–976. https://doi.org/10.1016/j.msec.2016.08.011.

Khampieng, T., Aramwit, P., Supaphol, P., 2015. Silk sericin loaded alginate nanoparticles: preparation and anti-inflammatory efficacy. Int. J. Biol. Macromol. 80, 636–643. https://doi.org/10.1016/j.ijbiomac.2015.07.018.

Khanal, S., Adhikari, U., Rijal, N.P., Bhattarai, S.R., Sankar, J., Bhattarai, N., 2016. pH-responsive PLGA nanoparticle for controlled payload delivery of diclofenac sodium. J. Funct. Biomater. 7, 21. https://doi.org/10.3390/jfb7030021.

Kloesch, B., Liszt, M., Broell, J., Steiner, G., 2011. Dimethyl sulphoxide and dimethyl sulphone are potent inhibitors of IL-6 and IL-8 expression in the human chondrocyte cell line C-28/I2. Life Sci. 89, 473–478. https://doi.org/10.1016/j.lfs.2011.07.015.

Liu, Q., Chen, J., Qin, Y., Jiang, B., Zhang, T., 2020. Zein/fucoidan-based composite nanoparticles for the encapsulation of pterostilbene: Preparation, characterization, physicochemical stability, and formation mechanism. Int. J. Biol. Macromol. 158, 461–470. https://doi.org/10.1016/j.ijbiomac.2020.04.128.

Liu, Q., Qin, Y., Jiang, B., Chen, J., Zhang, T., 2022b. Development of self-assembled zein-fucoidan complex nanoparticles as a delivery system for resveratrol. Colloids Surfaces B Biointerfaces 216, 112529. https://doi.org/10.1016/j.colsurfb.2022.112529.

Liu, D., Zhong, Z., Karin, M., 2022a. NF-κB: a double-edged sword controlling inflammation. Biomedicines 10, 1250. https://doi.org/10.3390/biomedicines10061250.

Luthuli, S., Wu, S., Cheng, Y., Zheng, X., Wu, M., Tong, H., 2019. Therapeutic effects of fucoidan: a review on recent studies. Mar. Drugs 17, 487. https://doi.org/10.3390/md17090487.

Ma, W., Wang, J., Wu, D., Chen, H., Wu, C., Du, M., 2020. The mechanism of improved thermal stability of protein-enriched O/W emulsions by soy protein particles. Food Funct. 11, 1385–1396. https://doi.org/10.1039/c9fo02270h.

Majumder, J., Minko, T., 2021. Multifunctional and stimuli-responsive nanocarriers for targeted therapeutic delivery. Expert Opin. Drug Deliv. 18, 205–227. https://doi.org/10.1080/17425247.2021.1828339.

McGettigan, P., Henry, D., 2013. Use of non-steroidal anti-inflammatory drugs that elevate cardiovascular risk: an examination of sales and essential medicines lists in low-, middle-, and high-income countries. PLoS Med. 10, e1001388.

Moore, N., Duong, M., Gulmez, S.E., Blin, P., Droz, C., 2019. Pharmacoepidemiology of non-steroidal anti-inflammatory drugs. Therapies 74, 271–277. https://doi.org/10.1016/j.therap.2018.11.002.

Mutukuri, T.T., Wilson, N.E., Taylor, L.S., Topp, E.M., Zhou, Q.T., 2021. Effects of drying method and excipient on the structure and physical stability of protein solids: Freeze drying vs. spray freeze drying. Int. J. Pharm. 594, 120169. doi: 10.1016/j.ijpharm.2020.120169.

Obluchinskaya, E.D., Pozharitskaya, O.N., Shikov, A.N., 2022. In vitro anti-inflammatory activities of fucoidans from five species of brown seaweeds. Mar. Drugs 20, 606. https://doi.org/10.3390/md20100606.

Öztürk, A.A., Namlı, İ., Güleç, K., Kıyan, H.T., 2020. Diclofenac sodium loaded PLGA nanoparticles for inflammatory diseases with high anti-inflammatory properties at low dose: formulation, characterization and in vivo HET-CAM analysis. Microvasc. Res. 130, 103991 https://doi.org/10.1016/j.mvr.2020.103991.

Panchal, N.K., Sabina, E.P., 2023. Non-steroidal anti-inflammatory drugs (NSAIDs): a current insight into its molecular mechanism eliciting organ toxicities. Food Chem. Toxicol. 113598 https://doi.org/10.1016/j.fct.2022.113598.

Park, H.Y., Han, M.H., Park, C., Jin, C.-Y., Kim, G.Y., Choi, I.W., Kim, N.D., Nam, T.J., Kwon, T.K., Choi, Y.H., 2011. Anti-inflammatory effects of fucoidan through inhibition of NF-κB, MAPK and Akt activation in lipopolysaccharide-induced BV2 microglia cells. Food Chem. Toxicol. 49, 1745–1752. https://doi.org/10.1016/j.fct.2011.04.020.

Pozharitskaya, O.N., Obluchinskaya, E.D., Shikov, A.N., 2020. Mechanisms of bioactivities of fucoidan from the brown seaweed Fucus vesiculosus L. of the Barents Sea. Mar. Drugs 18, 275. https://doi.org/10.3390/md18050275.

Pradhan, B., Patra, S., Nayak, R., Behera, C., Dash, S.R., Nayak, S., Sahu, B.B., Bhutia, S. K., Jena, M., 2020. Multifunctional role of fucoidan, sulfated polysaccharides in human health and disease: a journey under the sea in pursuit of potent therapeutic agents. Int. J. Biol. Macromol. 164, 4263–4278. https://doi.org/10.1016/j.ijbiomac.2020.09.019.

Radu, I.C., Zaharia, C., Hudiță, A., Tanasă, E., Ginghină, O., Marin, M., Gălățeanu, B., Costache, M., 2021. In vitro interaction of doxorubicin-loaded silk sericin nanocarriers with mcf-7 breast cancer cells leads to DNA damage. Polymers (basel). 13, 2047. https://doi.org/10.3390/polym13132047.

Rahimpour, S., Jabbari, H., Yousofi, H., Fathi, A., Mahmoodi, S., Jafarian, M.J., Shomali, N., Shotorbani, S.S., 2023. Regulatory effect of sericin protein in inflammatory pathways; a comprehensive review. Pathol. Pract. 154369 https://doi.org/10.1016/j.prp.2023.154369.

Rani, R., Raina, N., Sharma, A., Kumar, P., Tulli, H.S., Gupta, M., 2023. Advancement in nanotechnology for treatment of rheumatoid arthritis: scope and potential applications. Naunyn. Schmiedebergs. Arch. Pharmacol. 1–24 https://doi.org/10.1007/s00210-023-02514-5.

Reboredo, C., González-Navarro, C.J., Martínez-Oharriz, C., Martínez-López, A.L., Irache, J.M., 2021. Preparation and evaluation of PEG-coated zein nanoparticles for oral drug delivery purposes. Int. J. Pharm. 597, 120287 https://doi.org/10.1016/j.ijpharm.2021.120287.

Song, Y., Zhang, C., Zhang, J., Sun, N., Huang, K., Li, H., Wang, Z., Huang, K., Wang, L., 2016. An injectable silk sericin hydrogel promotes cardiac functional recovery after ischemic myocardial infarction. Acta Biomater. 41, 210–223. https://doi.org/10.1016/j.actbio.2016.05.039.

Sun, Y., Shi, W., Zhang, Q., Guo, H., Dong, Z., Zhao, P., Xia, Q., 2022. Multi-omics integration to reveal the mechanism of sericin inhibiting LPS-induced inflammation. Int. J. Mol. Sci. 24, 259. https://doi.org/10.1016/j.foodchem.2023.135982.

Sun, S., Zhang, X., Li, J., Li, Y., Zhou, C., Xiang, S., Tan, M., 2023. Preparation and evaluation of ovalbumin-fucoidan nanoparticles for nicotinamide mononucleotide encapsulation with enhanced stability and anti-aging activity. Food Chem. 418, 135982 https://doi.org/10.1016/j.foodchem.2023.135982.

Thorne, C., Boire, G., Chow, A., Garces, K., Liu, F., Poulin-Costello, M., Walker, V., Haraoui, B., 2017. Dose escalation and co-therapy intensification between etanercept, adalimumab, and infliximab: the CADURA study. Open Rheumatol. J. 11, 123. https://doi.org/10.2174/1874312901711010123.

Umerska, A., Paluch, K.J., Santos-Martinez, M.J., Corrigan, O.I., Medina, C., Tajber, L., 2018. Freeze drying of polyelectrolyte complex nanoparticles: effect of nanoparticle composition and cryoprotectant selection. Int. J. Pharm. 552, 27–38. https://doi.org/10.1016/j.ijpharm.2018.09.035.

Vaamonde-García, C., Florez-Fernandez, N., Torres, M.D., Lamas-Vazquez, M.J., Blanco, F.J., Domínguez, H., Meijide-Faílde, R., 2021. Study of fucoidans as natural biomolecules for therapeutical applications in osteoarthritis. Carbohydr. Polym. 258, 117692 https://doi.org/10.1016/j.carbpol.2021.117692.

Voci, S., Gagliardi, A., Salvatici, M.C., Fresta, M., Cosco, D., 2022. Influence of the dispersion medium and cryoprotectants on the physico-chemical features of gliadin- and zein-based Nanoparticles. Pharmaceutics 14, 332. https://doi.org/10.3390/pharmaceutics14020332.

Wang, J., Cheng, H., Chen, W., Han, P., Yao, X., Tang, B., Duan, W., Li, P., Wei, X., Chu, P.K., 2023. An injectable, self-healing composite hydrogel with enhanced near-infrared photo-antibacterial therapeutic effects for accelerated wound healing. Chem. Eng. J. 452, 139474 https://doi.org/10.1016/j.cej.2022.139474.

Wang, L., Yang, H.W., Ahn, G., Fu, X., Xu, J., Gao, X., Jeon, Y.J., 2021. In vitro and in vivo anti-inflammatory effects of sulfated polysaccharides isolated from the edible brown seaweed. Sargassum Fulvellum. Mar. Drugs 19, 277. https://doi.org/10.3390/md19050277.

Zayed, A., Ulber, R., 2019. Fucoidan production: approval key challenges and opportunities. Carbohydr. Polym. 211, 289–297. https://doi.org/10.1016/j.carbpol.2019.01.105.

Zhang, M., Hu, W., Cai, C., Wu, Y., Li, J., Dong, S., 2022. Advanced application of stimuli-responsive drug delivery system for inflammatory arthritis treatment. Mater. Today. Bio 14, 100223. https://doi.org/10.1016/j.mtbio.2022.100223.

Zhang, H., Jiang, L., Tong, M., Lu, Y., Ouyang, X.-K., Ling, J., 2021. Encapsulation of curcumin using fucoidan stabilized zein nanoparticles: preparation, characterization, and in vitro release performance. J. Mol. Liq. 329, 115586 https://doi.org/10.1016/j.molliq.2021.115586.

Zhang, X.Q., Xu, X., Bertrand, N., Pridgen, E., Swami, A., Farokhzad, O.C., 2012. Interactions of nanomaterials and biological systems: implications to personalized nanomedicine. Adv. Drug Deliv. Rev. 64, 1363–1384. https://doi.org/10.1016/j.addr.2012.08.005.

Zhu, J.J., Tang, C.H., Luo, F.C., Yin, S.W., Yang, X.Q., 2022. Topical application of zein-silk sericin nanoparticles loaded with curcumin for improved therapy of dermatitis. Mater. Today Chem. 24, 100802 https://doi.org/10.1016/j.mtchem.2022.100802.